

# Sparsity by Worst-Case Penalties

Yves Grandvalet<sup>a</sup>, Julien Chiquet<sup>b</sup>, Christophe Ambroise<sup>c</sup>

<sup>a</sup>*Sorbonne universités, Université de technologie de Compiègne, CNRS, Heudiasyc UMR 7253, CS 60 319, 60 203 Compiègne cedex, France*

<sup>b</sup>*AgroParisTech, INRA, Université Paris-Saclay*

*UMR MIA-Paris, 16 rue Claude Bernard, 75005, Paris, France*

<sup>c</sup>*Université d'Évry Val d'Essonne, Université Paris-Saclay, ENSIE, USC INRA UMR CNRS 8071, LaMME, 91000 Évry, France*

---

## Abstract

This paper proposes a new interpretation of sparse penalties such as the elastic-net and the group-lasso. Beyond providing a new viewpoint on these penalization schemes, our approach results in a unified optimization strategy. Our experiments demonstrate that this strategy, implemented on the elastic-net, is computationally extremely efficient for small to medium size problems. Our accompanying software solves problems very accurately, at machine precision, in the time required to get a rough estimate with competing state-of-the-art algorithms. We illustrate on real and artificial datasets that this accuracy is required to for the correctness of the support of the solution, which is an important element for the interpretability of sparsity-inducing penalties.

*Keywords:* sparsity, adaptive penalty, dual norm, optimality gap

---

## 1. Introduction

Inferential statistics aim at drawing conclusions from data and from some kind of assumption or prior information about the underlying distribution. It is well known that processes where data guide the choice of assumptions can lead to paradoxes, resulting from overfitting issues, in particular in the large dimensional setup when data are used to select explicative variables: the seeming explanatory power of weakly relevant variables can be important when the number of variables is similar to the number of data points (Freedman, 1983; Ambroise and McLachlan, 2002). In this context, we present here an unusual reformulation of variable selection methods based on sparsity-inducing penalties: we show that these methods can be interpreted as adaptive penalties, where adaptivity refers to the choice of the eventual penalty from data. However, contrary to the available reformulations so far, ours shows that the adaptation of the sparsity-inducing penalty to data follows a disagreement principle, where the least-favorable penalty is selected from data.

We believe that our new viewpoint can be instrumental in unified analyses of algorithms and their derived estimators, and we show here two such examples: first, we provide a generic algorithm for solving the data fitting problem; then, we derive the general form of an optimality gap

---

*Email addresses:* [yves.grandvalet@utc.fr](mailto:yves.grandvalet@utc.fr) (Yves Grandvalet), [julien.chiquet@inra.fr](mailto:julien.chiquet@inra.fr) (Julien Chiquet), [christophe.ambroise@genopole.cnrs.fr](mailto:christophe.ambroise@genopole.cnrs.fr) (Christophe Ambroise)

*Preprint submitted to arXiv*

*July 20, 2017*

that may be used to monitor convergence. Our experimental section illustrates the effectiveness of the generic algorithm motivated by our interpretation, when instanced on the elastic-net estimator: the algorithm, which relies on solving linear systems is accurate, and computationally efficient up to medium scale problems (thousands of variables). As a side experimental result, we show that solving problems with high precision, as with the proposed approach, benefits to the performances, either measured in terms of prediction accuracy or in terms of support error rate.

## 2. Adaptive Penalties

### 2.1. Background

We consider the linear regression model

$$Y = X\boldsymbol{\beta}^* + \varepsilon , \quad (1)$$

where  $Y$  is a continuous response variable,  $X = (X_1, \dots, X_p)$  is a vector of  $p$  predictor variables,  $\boldsymbol{\beta}^*$  is the vector of unknown parameters and  $\varepsilon$  is a zero-mean Gaussian error variable with variance  $\sigma^2$ . We will assume throughout this paper that  $\boldsymbol{\beta}^*$  has few non-zero coefficients.

The estimation and inference of  $\boldsymbol{\beta}^*$  is based on training data, consisting of a vector  $\mathbf{y} = (y_1, \dots, y_n)^\top$  for responses and a  $n \times p$  design matrix  $\mathbf{X}$  whose  $j$ th column contains  $\mathbf{x}_j = (x_j^1, \dots, x_j^n)^\top$ , the  $n$  observations for variable  $X_j$ . For clarity, we assume that both  $\mathbf{y}$  and  $\{\mathbf{x}_j\}_{j=1, \dots, p}$  are centered so as to eliminate the intercept from fitting criteria.

Penalization methods that build on the  $\ell_1$ -norm, referred to as *Lasso* procedures (Least Absolute Shrinkage and Selection Operator), are now widely used to tackle simultaneously variable estimation and selection in sparse problems. They define a shrinkage estimator of the form

$$\hat{\boldsymbol{\beta}} = \arg \min_{\boldsymbol{\beta} \in \mathbb{R}^p} \frac{1}{2} \|\mathbf{X}\boldsymbol{\beta} - \mathbf{y}\|_2^2 + \lambda \|\boldsymbol{\beta}\| , \quad (2)$$

where  $\|\cdot\|_2$  is the Euclidean norm and  $\|\cdot\|$  is an arbitrary norm, chosen to induce some assumed sparsity pattern (typically  $\ell_1$  or  $\ell_{c,1}$  norms, where  $c \in (1, \infty]$ ).

The existence of computationally efficient optimization procedures plays an important role in the popularity of these methods. Although various general-purpose convex optimization solvers could be used (Boyd and Vandenberghe, 2004), exploiting the structure of the regularization problem – especially the sparsity of solutions – is essential in terms of computational efficiency. Bach et al. (2012) provided an overview of the families of techniques specifically designed for solving this type of problems: proximal methods, coordinate descent algorithms, reweighted- $\ell_2$  algorithms, working-set methods. Stochastic gradient methods (Moulines and Bach, 2011), the Frank-Wolfe algorithm (Lacoste-Julien et al., 2012) or ADMM (Alternating Direction Method of Multipliers, Boyd et al., 2011) have also recently gained in popularity to the resolution of sparse problems.

We present below a new formulation of Problem (2) that motivates an algorithm that may seem reminiscent of reweighted- $\ell_2$  algorithms, but which is in fact more closely related to working-set methods. As for reweighted- $\ell_2$  algorithms, our proposal is based on the reformulation of the sparsity-inducing penalty in terms of penalties that are simpler to handle (linear or quadratic). However, whereas reweighted- $\ell_2$  algorithms rely on a variational formulation of the sparsity-inducing norm that ends up in an augmented minimization problem, our proposal is rooted in the duality principle, eventually leading to a minimax problem that lends itself to a working-set algorithm that will be presented in Section 4.

## 2.2. Dual Norms

When the sparsity-inducing penalty is a norm, its sublevel sets can always be defined as the intersection of linear or quadratic sublevel sets. In other words, if the optimization problem is written in the form of a constrained optimization problem with inequality constraints pertaining to the penalty, then, the feasible region can be defined as the intersection of linear or quadratic regions. This fact, which is illustrated in Figures 2 and 3, stems from the definition of dual norms:

$$\|\boldsymbol{\beta}\| = \max_{\boldsymbol{\gamma} \in \mathcal{B}_*^1} \boldsymbol{\gamma}^\top \boldsymbol{\beta} ,$$

where  $\mathcal{B}_*^1$  is the unit ball centered at the origin defined from the dual norm  $\|\cdot\|_*$ , i.e.  $\mathcal{B}_*^1 = \{\boldsymbol{\gamma} \in \mathbb{R}^p : \|\boldsymbol{\gamma}\|_* \leq 1\}$ . Using this definition, Problem (2) can be reformulated as

$$\hat{\boldsymbol{\beta}} = \arg \min_{\boldsymbol{\beta} \in \mathbb{R}^p} \max_{\boldsymbol{\gamma} \in \mathcal{B}_*^1} \frac{1}{2} \|\mathbf{X}\boldsymbol{\beta} - \mathbf{y}\|_2^2 + \lambda \boldsymbol{\gamma}^\top \boldsymbol{\beta} . \quad (3)$$

Technically, this formulation is the primal form of the original Problem (2) using the coupling function defined by the dual norm (see e.g. Gilbert, 2016; Bonnans et al., 2006). It is interesting in the sense that the problem

$$\min_{\boldsymbol{\beta} \in \mathbb{R}^p} \frac{1}{2} \|\mathbf{X}\boldsymbol{\beta} - \mathbf{y}\|_2^2 + \lambda \boldsymbol{\gamma}^\top \boldsymbol{\beta}$$

is simple to solve for any value of  $\boldsymbol{\gamma}$ , since it only requires solving a linear system. Indeed, the problem

$$\begin{aligned} \hat{\boldsymbol{\gamma}} &= \arg \max_{\boldsymbol{\gamma} \in \mathcal{B}_*^1} \frac{1}{2} \|\mathbf{X}\boldsymbol{\beta} - \mathbf{y}\|_2^2 + \lambda \boldsymbol{\gamma}^\top \boldsymbol{\beta} \\ &= \arg \max_{\boldsymbol{\gamma} \in \mathcal{B}_*^1} \boldsymbol{\gamma}^\top \boldsymbol{\beta} \end{aligned} \quad (4)$$

is usually straightforward to solve. Besides the sparsity of  $\hat{\boldsymbol{\beta}}$ , the overall efficiency of our algorithm relies also on the invariance of  $\hat{\boldsymbol{\gamma}}$  with respect to large changes in  $\boldsymbol{\beta}$ . For the penalties we are interested in,  $\hat{\boldsymbol{\gamma}}$  takes its value in a finite set, defined by the extreme points of the convex polytope  $\mathcal{B}_*^1$ . This number of points typically increases exponentially in  $p$ , but, with the working-set strategy, the number of configuration actually visited typically grows linearly with the number of non-zero coefficients in the solution  $\hat{\boldsymbol{\beta}}$ .

## 2.3. Relations with Other Methods

The expansion in dual norm expressed in Problem (3) bears some similarities with the first step of the derivation of very general duality schemes, such as Fenchel's duality or Lagrangian duality. It is however dedicated to the category of problems expressed as in (2), thereby offering an interesting novel view of this category of problems. In particular, it provides geometrical insights on these methods and a generic algorithm for computing solutions. The associated algorithm, that relies on solving linear systems is accurate, and efficient up to medium scale problems (thousands of variables).

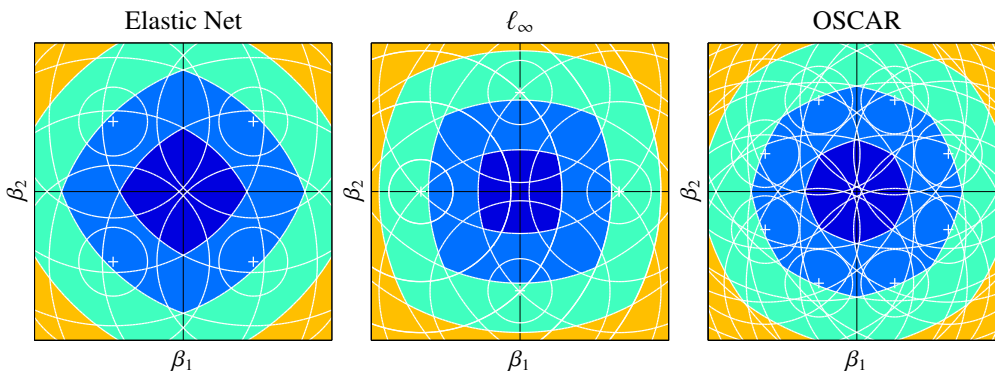


Figure 1: Sublevel sets for several penalties (represented by the colored patches). Each set is defined as the intersection of the the Euclidean balls whose boundaries are represented by white circles, and whose centers are represented by white crosses.

#### 2.4. Geometrical Interpretation

Geometrical insights are easier to gain from a slightly different formulation of Problem (3):<sup>1</sup>

$$\min_{\beta \in \mathbb{R}^p} \max_{\gamma \in \mathcal{B}_*^\eta} \frac{1}{2} \|\mathbf{X}\beta - \mathbf{y}\|_2^2 + \frac{\lambda}{2} \|\beta - \gamma\|_2^2 . \quad (5)$$

The penalty  $\lambda \|\beta - \gamma\|_2^2$  corresponds to a hard constraint  $\|\beta - \gamma\|_2^2 \leq c$ , which states that the solution in  $\beta$  belongs to a  $\ell_2$  ball centered in  $\gamma$ . Then, as  $\hat{\gamma}$  maximizes  $\|\hat{\beta} - \gamma\|_2^2$ , the solution  $\hat{\beta}$  belongs to the intersection of all the balls centered in  $\gamma \in \mathcal{B}_*^\eta$ . Eventually, the active constraints will be defined by the  $\gamma$  values for which  $\|\hat{\beta} - \gamma\|_2^2$  is maximal, that is for the worst-case  $\hat{\gamma}$  values. For the penalties we are interested in,  $\hat{\gamma}$  takes its value in a finite set, defined by the extreme points of the convex polytope  $\mathcal{B}_*^\eta$ . This is the case for the Lasso, the  $\ell_{1,\infty}$  version of the group-lasso (where the magnitude of regression coefficients are assumed to be equal within groups, either zero or non-zero), and for OSCAR (Octagonal Shrinkage and Clustering Algorithm for Regression) which is based on a penalizer encouraging the sparsity of the regression coefficients and the equality of the non-zero entries (Bondell and Reich, 2008). Figure 1 illustrates those three sparse problems with their associated worst case quadratic penalty.

### 3. Worst-Case Quadratic Penalties

Our framework is amenable to many variations. Here, we present two examples where the desired penalty on the regression coefficients  $\beta$  is implemented through the definition of the dual norm on the coefficients  $\gamma$ . When the desired penalty on  $\beta$  is expressed by  $\ell_1$  or  $\ell_\infty$  norms, this process results in unit balls  $\mathcal{B}_*^\eta$  which are convex polytopes that are easy to manage when solving Problem (5), since they can be defined as the convex hulls of a finite number of values.

The two sparsity-inducing penalizers presented below have a grouping effect. The elastic-net implements this grouping without predefining the group structure: strongly correlated predictors

<sup>1</sup>This quadratic formulation is more general, in the sense that it corresponds to Problem (3) with a proper rescaling of  $\lambda$  in the limit of  $\eta \rightarrow +\infty$ .

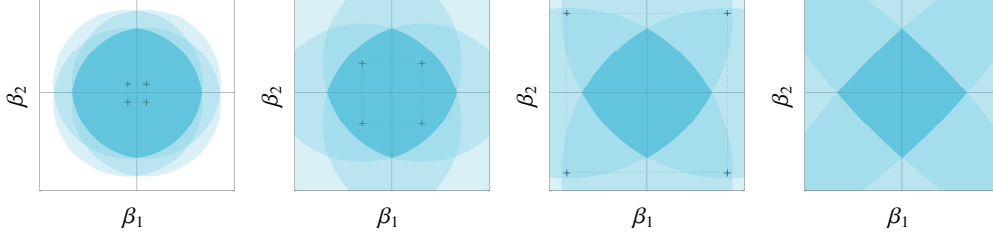


Figure 2: Sublevel sets for elastic net penalties (represented by the darker colored patches). Each set is defined as the intersection of the the Euclidean balls (represented by the lighter color patches) whose centers are represented by crosses.

tend to be in or out of the model together (Zou and Hastie, 2005). The  $\ell_{\infty,1}$  group-Lasso that is presented subsequently is based on a prescribed group structure and favors regression coefficients with identical magnitude within activated groups.

### 3.1. Elastic-Net

As an introductory example, let us consider the assumption stating that the  $\ell_1$ -norm of  $\beta^*$  should be small. The dual norm is the  $\ell_\infty$ -norm:

$$\begin{aligned} \mathcal{B}_*^\eta &= \left\{ \gamma \in \mathbb{R}^p : \sup_{\|\beta\|_1 \leq 1} \gamma^\top \beta \leq \eta \right\} \\ &= \{ \gamma \in \mathbb{R}^p : \|\gamma\|_\infty \leq \eta \} \\ &= \mathbf{conv}\{ \{-\eta, \eta\}^p \} , \end{aligned}$$

where  $\mathbf{conv}$  denotes convex hull, so that Problem (5) reads:

$$\begin{aligned} & \min_{\beta \in \mathbb{R}^p} \max_{\gamma \in \mathcal{B}_*^\eta} \left\{ \frac{1}{2} \|\mathbf{X}\beta - \mathbf{y}\|_2^2 + \frac{\lambda}{2} \|\beta - \gamma\|_2^2 \right\} \\ \Leftrightarrow & \min_{\beta \in \mathbb{R}^p} \frac{1}{2} \|\mathbf{X}\beta - \mathbf{y}\|_2^2 + \lambda \eta \|\beta\|_1 + \frac{\lambda}{2} \|\beta\|_2^2 , \end{aligned} \quad (6)$$

which is recognized as an elastic-net problem. When  $\eta$  is null, we recover ridge regression, and when  $\eta$  goes to infinity, the problem approaches a Lasso problem. A 2D pictorial illustration of this evolution is given in Figure 2, where the shape of the uncertainty set  $\mathcal{B}_*^\eta$  is the convex hull of the points located at  $(\pm\eta, \pm\eta)^\top$ , which are identified by the cross markers. Then, the sublevel set  $\{\beta : \max_{\gamma \in \mathcal{B}_*^\eta} \|\beta - \gamma\|_2^2 \leq t\}$  is simply defined as the intersection of the four sublevel sets  $\{\beta : \|\beta - \gamma\|_2^2 \leq t\}$  for  $\gamma = (\pm 1, \pm 1)^\top$ , which are Euclidean balls centered at these  $\gamma$  values.

### 3.2. Group-Lasso

We consider here the  $\ell_{\infty,1}$  variant of the group-Lasso, which was first proposed by Turlach et al. (2005) to perform variable selection in the multiple response setup. A group structure is defined on the set of variables by setting a partition of the index set  $\mathcal{I} = \{1, \dots, p\}$ , that is,  $\mathcal{I} = \bigcup_{k=1}^K \mathcal{G}_k$ , with  $\mathcal{G}_k \cap \mathcal{G}_\ell = \emptyset$  for  $k \neq \ell$ . Let  $p_k$  denote the cardinality of group  $k$ , and  $\beta_{\mathcal{G}_k} \in \mathbb{R}^{p_k}$  be the vector  $(\beta_j)_{j \in \mathcal{G}_k}$ .

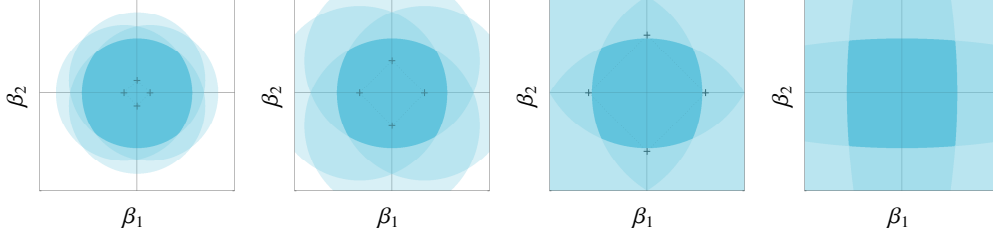


Figure 3: Sublevel sets for the  $\ell_{\infty,1}$  group-Lasso penalties (represented by the darker colored patches). Each set is defined as the intersection of the the Euclidean balls (represented by the lighter color patches) whose centers are represented by crosses.

The  $\ell_{\infty,1}$  mixed-norm of  $\boldsymbol{\beta}$  (that is, its groupwise  $\ell_{\infty}$ -norm) is defined as

$$\mathcal{B} = \left\{ \boldsymbol{\beta} \in \mathbb{R}^p : \sum_{k=1}^K \|\boldsymbol{\beta}_{\mathcal{G}_k}\|_{\infty} \leq 1 \right\} .$$

The dual norm is the groupwise  $\ell_1$ -norm:

$$\begin{aligned} \mathcal{B}_*^{\eta} &= \left\{ \boldsymbol{\gamma} \in \mathbb{R}^p : \sup_{\boldsymbol{\beta} \in \mathcal{B}} \boldsymbol{\gamma}^{\top} \boldsymbol{\beta} \leq \eta \right\} \\ &= \left\{ \boldsymbol{\gamma} \in \mathbb{R}^p : \max_{k \in \{1, \dots, K\}} \|\boldsymbol{\gamma}_{\mathcal{G}_k}\|_1 \leq \eta \right\} \\ &= \text{conv} \left\{ \eta \mathbf{e}_1^{p_1}, \dots, \eta \mathbf{e}_{p_1}^{p_1}, -\eta \mathbf{e}_1^{p_1}, \dots, -\eta \mathbf{e}_{p_1}^{p_1} \right\} \times \dots \\ &\quad \times \left\{ \eta \mathbf{e}_1^{p_K}, \dots, \eta \mathbf{e}_{p_K}^{p_K}, -\eta \mathbf{e}_1^{p_K}, \dots, -\eta \mathbf{e}_{p_K}^{p_K} \right\} , \end{aligned}$$

where  $\mathbf{e}_j^p$  is the  $j$ th element of the canonical basis of  $\mathbb{R}^p$ . Problem (5) becomes:

$$\begin{aligned} &\min_{\boldsymbol{\beta} \in \mathbb{R}^p} \max_{\boldsymbol{\gamma} \in \mathcal{B}_*^{\eta}} \left\{ \frac{1}{2} \|\mathbf{X}\boldsymbol{\beta} - \mathbf{y}\|_2^2 + \frac{\lambda}{2} \|\boldsymbol{\beta} - \boldsymbol{\gamma}\|_2^2 \right\} \\ &\Leftrightarrow \min_{\boldsymbol{\beta} \in \mathbb{R}^p} \frac{1}{2} \|\mathbf{X}\boldsymbol{\beta} - \mathbf{y}\|_2^2 + \lambda \eta \sum_{k=1}^K \|\boldsymbol{\beta}_{\mathcal{G}_k}\|_{\infty} + \frac{\lambda}{2} \|\boldsymbol{\beta}\|_2^2 , \end{aligned}$$

Notice that the limiting cases of this penalty are two classical problems: ridge regression and the  $\ell_{\infty,1}$  group-Lasso. A 2D pictorial illustration of this evolution is given in Figure 3, where  $\mathcal{B}_*^{\eta}$  is the convex hull of the points located on the axes at  $\pm\eta$ , which are identified by the cross markers. Then, the sublevel set  $\{\boldsymbol{\beta} : \max_{\boldsymbol{\gamma} \in \mathcal{B}_*^{\eta}} \|\boldsymbol{\beta} - \boldsymbol{\gamma}\|_2^2 \leq t\}$  is simply defined as the intersection of the four sublevel sets  $\{\boldsymbol{\beta} : \|\boldsymbol{\beta} - \boldsymbol{\gamma}\|_2^2 \leq t\}$  for  $\boldsymbol{\gamma} = \pm\eta \mathbf{e}_1^2$  and  $\boldsymbol{\gamma} = \pm\eta \mathbf{e}_2^2$ , which are Euclidean balls centered at these  $\boldsymbol{\gamma}$  values.

#### 4. Algorithm

The unified derivation for the problems presented in Section 3 suggests a unified processing based on the iterative resolution of quadratic problems. This general algorithm is summarized

in this section. We then show that the new derivation can also be used in the analysis of this algorithm by describing an alternative to Fenchel duality (used for example by Bach et al., 2012) to assess convergence.

#### 4.1. Active Set Approach

The efficient approaches developed for sparse regression take advantage of the sparsity of the solution by solving a series of small linear systems, the sizes of which are incrementally increased/decreased. Here, as for the Lasso (Osborne et al., 2000; Efron et al., 2004), this process boils down to an iterative optimization scheme involving the resolution of quadratic problems.

The algorithm is based on the iterative update of the set of “active” variables,  $\mathcal{A}$ , indexing the coefficients  $\beta_{\mathcal{A}}$  currently identified as being non-zero. It is started from a sparse initial guess, say  $\mathcal{A} = \emptyset$  ( $\beta = 0$ ), and iterates the three following steps:

1. the first step solves Problem (5) considering that  $\mathcal{A}$ , the set of “active” variables, is correct; that is, the objective (5) is optimized with respect to  $\beta_{\mathcal{A}}$ . This penalized least squares problem is defined from  $\mathbf{X}_{\cdot,\mathcal{A}}$ , which is the submatrix of  $\mathbf{X}$  comprising all rows and the columns indexed by  $\mathcal{A}$  and  $\gamma_{\mathcal{A}}$ , which is set to its current most adversarial value.<sup>2</sup>
2. the second step updates  $\beta_{\mathcal{A}}$  if necessary (and possibly  $\gamma_{\mathcal{A}}$ ), so that  $\gamma_{\mathcal{A}}$  is indeed (one of) the most adversarial value of the current  $\beta_{\mathcal{A}}$ . This is easily checked with the problems given in Section 3, where  $\mathcal{B}_*^{\eta}$  is a convex polytope whose vertices (that is, extreme  $\gamma$ -values) are associated with a cone of coherent  $\beta$ -value.
3. the last step updates the active set  $\mathcal{A}$ . It relies on the “worst-case gradient” with respect to  $\beta$ , where  $\gamma$  is chosen so as to minimize infinitesimal improvements of the current solution. Again picking the right  $\gamma$  is easy for the problems given in Section 3. Once this is done, we first check whether some variables should quit the active set, and if this is not the case, we assess the completeness of  $\mathcal{A}$ , by checking the optimality conditions with respect to inactive variables. We add the variable, or the group of variables that most violates the worst-case optimality conditions. When no such violation exists, the current solution is optimal, since, at this stage, the problem is solved exactly within the active set  $\mathcal{A}$ .

Algorithm 1 provides a more comprehensive technical description.

Note that the structure is essentially identical to the one proposed by Osborne et al. (2000) or Efron et al. (2004) for the Lasso, but that it applies to any penalty that can be decomposed as in Problem (5). Our viewpoint is also radically different, as the global non-smooth problem is dealt with subdifferentials by Osborne et al. (2000), whereas we rely on the maximum of smooth functions. This approach suggests a new assessment of convergence, as detailed below.

#### 4.2. Monitoring Convergence

At each iteration of the algorithm, the current  $\beta$  is computed assuming that the current active set  $\mathcal{A}$  and the current  $\gamma_{\mathcal{A}}$ -value are optimal. When the current active set is not optimal, the current  $\beta$  (where  $\beta_{\mathcal{A}}$  is completed by zeros on the complement  $\mathcal{A}^c$ ) is nevertheless optimal for a  $\gamma$ -value defined in  $\mathbb{R}^p$  (where  $\gamma_{\mathcal{A}}$  is completed by ad hoc values on the complement  $\mathcal{A}^c$ ). However this  $\gamma$  fails to belong to  $\mathcal{B}_*^{\eta}$  (otherwise, the problem would be solved:  $\mathcal{A}$ ,  $\gamma$  and  $\beta$  would indeed be optimal). The following proposition relates the current objective function, associated with an infeasible  $\gamma$ -value ( $\gamma \notin \mathcal{B}_*^{\eta}$ ), to the global optimum of the optimization problem.

---

<sup>2</sup>When several  $\gamma_{\mathcal{A}}$  are equally unfavorable to  $\beta_{\mathcal{A}}$ , we use gradient information to pick the worst one among those when  $\beta_{\mathcal{A}}$  moves along the steepest descent direction.

---

**Algorithm 1: Worst-Case Active Set Algorithm**


---

```

Init.  $\beta \leftarrow \beta^0$ 
      Determine the active set:  $\mathcal{A} \leftarrow \{j : \beta_j > 0\}$ 
      Pick a worst admissible  $\gamma$ , that is,  $\gamma \in \arg \max_{\gamma' \in \mathcal{B}_*^l} \|\gamma' - \beta\|_2^2$ 

Step 1 Update active variables  $\beta_{\mathcal{A}}$  assuming that  $\mathcal{A}$  and  $\gamma_{\mathcal{A}}$  are optimal
       $\beta_{\mathcal{A}}^{\text{old}} \leftarrow \beta_{\mathcal{A}}$ 
       $\beta_{\mathcal{A}} \leftarrow (\mathbf{X}_{\mathcal{A}}^\top \mathbf{X}_{\mathcal{A}} + \lambda \mathbf{I}_{|\mathcal{A}|})^{-1} (\mathbf{X}_{\mathcal{A}}^\top \mathbf{y} - \lambda \gamma_{\mathcal{A}})$ 

Step 2 Verify coherence of  $\gamma_{\mathcal{A}}$  with the updated  $\beta_{\mathcal{A}}$ 
      if  $\|\beta_{\mathcal{A}} - \gamma_{\mathcal{A}}\|_2^2 < \max_{\mathbf{g} \in \mathcal{B}_*^l} \|\beta_{\mathcal{A}} - \mathbf{g}\|_2^2$  then // if  $\gamma_{\mathcal{A}}$  is not worst-case
      |   /* Backtrack towards the last  $\gamma_{\mathcal{A}}$ -coherent solution: */
      |    $\beta_{\mathcal{A}} \leftarrow \beta_{\mathcal{A}}^{\text{old}} + \rho(\beta_{\mathcal{A}} - \beta_{\mathcal{A}}^{\text{old}})$ 
      |    $\gamma_{\mathcal{A}}$  is worst-case for  $\beta_{\mathcal{A}}$ , and there is another worst-case value  $\tilde{\gamma}_{\mathcal{A}}$ 
      |   /* Check whether progress can be made with  $\tilde{\gamma}_{\mathcal{A}}$  */
      |    $\tilde{\beta}_{\mathcal{A}} \leftarrow (\mathbf{X}_{\mathcal{A}}^\top \mathbf{X}_{\mathcal{A}} + \lambda \mathbf{I}_{|\mathcal{A}|})^{-1} (\mathbf{X}_{\mathcal{A}}^\top \mathbf{y} - \lambda \tilde{\gamma}_{\mathcal{A}})$ 
      |   if  $\|\tilde{\beta}_{\mathcal{A}} - \tilde{\gamma}_{\mathcal{A}}\|_2^2 = \max_{\mathbf{g} \in \mathcal{B}_*^l} \|\tilde{\beta}_{\mathcal{A}} - \mathbf{g}\|_2^2$  then // if  $\tilde{\gamma}_{\mathcal{A}}$  is worst-case...
      |   |    $(\beta_{\mathcal{A}}, \gamma_{\mathcal{A}}) \leftarrow (\tilde{\beta}_{\mathcal{A}}, \tilde{\gamma}_{\mathcal{A}})$  //  $(\tilde{\beta}_{\mathcal{A}}, \tilde{\gamma}_{\mathcal{A}})$  is better than  $(\beta_{\mathcal{A}}, \gamma_{\mathcal{A}})$ 
      |   /* The current  $\gamma_{\mathcal{A}}$  is coherent with  $\beta_{\mathcal{A}}$  */

Step 3 Update active set  $\mathcal{A}$ 
       $g_j \leftarrow \min_{\gamma \in \mathcal{B}_*^l} |\mathbf{x}_j^\top (\mathbf{X}_{\mathcal{A}} \beta_{\mathcal{A}} - \mathbf{y}) + \lambda(\beta_j - \gamma_j)| \quad j = 1, \dots, p$  // worst-case gradient
      if  $\exists j \in \mathcal{A} : \beta_j = 0$  and  $g_j = 0$  then
      |    $\mathcal{A} \leftarrow \mathcal{A} \setminus \{j\}$ ; // Downgrade  $j$ 
      |   /* Go to Step 1 */
      else
      |   if  $\max_{j \in \mathcal{A}^c} g_j \neq 0$  then
      |   |   /* Identify the greatest violation of optimality conditions */
      |   |    $j^* \leftarrow \arg \max_{j \in \mathcal{A}^c} g_j, \quad \mathcal{A} \leftarrow \mathcal{A} \cup \{j^*\}$ ; // Upgrade  $j^*$ 
      |   |   /* Go to Step 1 */
      |   else
      |   |   /* Stop and return  $\beta$ , which is optimal */

```

---

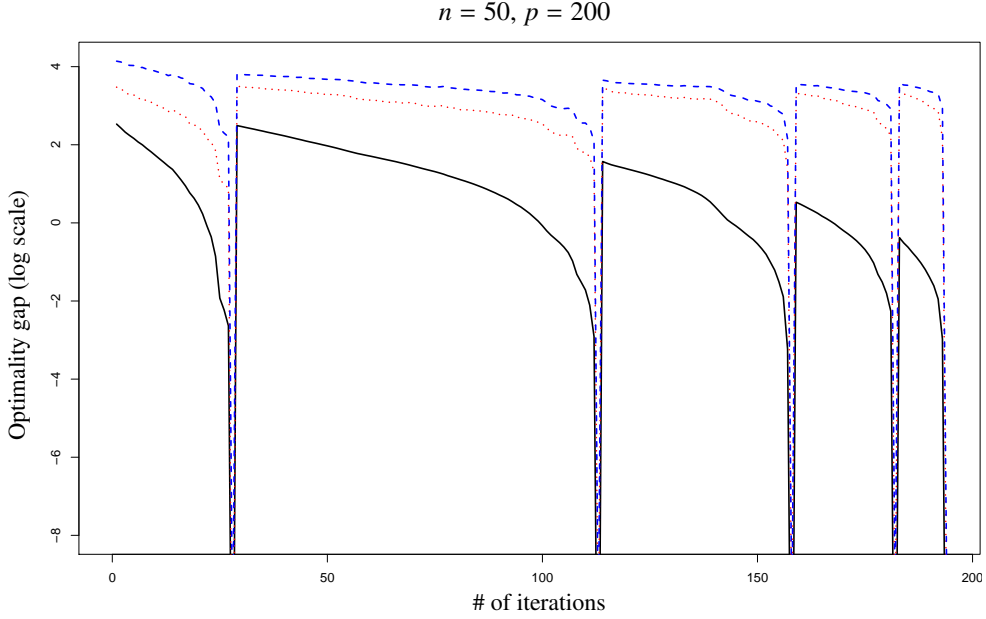


Figure 4: Monitoring convergence: true optimality gap (solid black) versus our generic upper bound (dashed blue) and Fenchel's duality gap for elastic net (dotted red) computed at each iteration of Algorithm 1.

**Proposition 1.** For any vectorial norm  $\|\cdot\|_*$ ,  $\forall \boldsymbol{\gamma} \in \mathbb{R}^p : \|\boldsymbol{\gamma}\|_* \geq \eta$ , we have:

$$\min_{\boldsymbol{\beta} \in \mathbb{R}^p} \max_{\boldsymbol{\gamma}' \in \mathcal{B}_*} J_\lambda(\boldsymbol{\beta}, \boldsymbol{\gamma}') \geq \frac{\eta}{\|\boldsymbol{\gamma}\|_*} J_\lambda(\boldsymbol{\beta}^*(\boldsymbol{\gamma}), \boldsymbol{\gamma}) - \frac{\lambda\eta(\|\boldsymbol{\gamma}\|_* - \eta)}{\|\boldsymbol{\gamma}\|_*^2} \|\boldsymbol{\gamma}\|_2^2 ,$$

where

$$J_\lambda(\boldsymbol{\beta}, \boldsymbol{\gamma}) = \|\mathbf{X}\boldsymbol{\beta} - \mathbf{y}\|_2^2 + \lambda \|\boldsymbol{\beta} - \boldsymbol{\gamma}\|_2^2 \quad \text{and} \quad \boldsymbol{\beta}^*(\boldsymbol{\gamma}) = \arg \min_{\boldsymbol{\beta} \in \mathbb{R}^p} J_\lambda(\boldsymbol{\beta}, \boldsymbol{\gamma}) .$$

See proof in Appendix A.

This proposition can be used to compute an optimality gap at Step 3 of Algorithm 1, by picking a  $\boldsymbol{\gamma}$ -value such that the current worst-case gradient  $\mathbf{g}$  is null (the current  $\boldsymbol{\beta}$ -value then being the optimal  $\boldsymbol{\beta}^*(\boldsymbol{\gamma})$ ). Note that more precise upper bounds could be computed relying on significant extra computation. The generic optimality gap computed from Proposition 1 differs from the Fenchel duality gap (see Bach et al., 2012). For the elastic net expressed in (6), Fenchel inequality (see details in Mairal, 2010) yields the following optimality gap:

$$\begin{aligned} \min_{\boldsymbol{\beta} \in \mathbb{R}^p} \max_{\boldsymbol{\gamma}' \in \mathcal{B}_*} J_\lambda(\boldsymbol{\beta}, \boldsymbol{\gamma}') &\geq J_\lambda(\boldsymbol{\beta}^*(\boldsymbol{\gamma}), \boldsymbol{\gamma}) - \frac{\eta^2}{\|\boldsymbol{\gamma}\|_*^2} \left( \|\mathbf{X}\boldsymbol{\beta}^*(\boldsymbol{\gamma}) - \mathbf{y}\|_2^2 + \lambda \|\boldsymbol{\beta}^*(\boldsymbol{\gamma})\|_2^2 \right) \\ &\quad - \frac{2\eta}{\|\boldsymbol{\gamma}\|_*} (\mathbf{X}\boldsymbol{\beta}^*(\boldsymbol{\gamma}) - \mathbf{y})^\top \mathbf{y} . \end{aligned}$$

The two optimality gaps are empirically compared in Figure 4 for the elastic net, along a short regularization path with five values of the  $\ell_1$ -penalization parameter. We see that the two options can be used to assess convergence, though Fenchel's duality gap is more accurate for the rougher

solutions. Note however that both upper bounds are fairly coarse until a very accurate solution is reached, which makes them both unsuitable for deriving loose stopping criteria. Proposition 1 is thus of limited scope, but it illustrates that, besides its algorithmic consequences, our original view of sparse penalties opens new ways for analysis. As a final note on this topic, we provide a slightly tighter inequality for computing the optimality gap in Appendix A, and we conjecture that it could be further tightened (see in particular the derivation of inequality (A.3)).

## 5. Numerical Experiments

This section compares the performances of our algorithm to its state-of-the-art competitors from an optimization viewpoint. Efficiency may then be assessed by accuracy and speed: accuracy is the difference between the optimum of the objective function and its value at the solution returned by the algorithm; speed is the computing time required for returning this solution. Obviously, the timing of two algorithms/packages has to be compared at similar precision requirements, which are rather crude in statistical learning, far from machine precision (Bottou and Bousquet, 2008).

We start by showing an experiment on a real dataset illustrating that optimization is an actual issue from the data analysis viewpoint. We then provide an in-depth analysis on simulated data, thereby covering a wide range of well-controlled situations, where our conclusions are derived from numerous simulations. Finally, the available ground truths will also be useful to show that optimization issues during training have notable effects in terms of prediction accuracy and support recovery.

### 5.1. Introductory Example: Quantitative Trait Loci and Association Mapping

Many quantitative traits in plants and animals are heritable. When considering Mendelian traits, the Quantitative Trait Loci (QTL) are sections of DNA that explain the trait variability. As traits are typically controlled by several QTL, the association between traits and QTL involves several limited effects that are difficult to detect individually.

A possible method for mapping genotype to trait consists in regressing the trait (that is, phenotype) of interest against the QTL (that is, genotype), using penalized regression. In this introductory example, we consider the maize association mapping panel described in (Rincent et al., 2014), where 269 individuals were genotyped with a 50k single-nucleotide polymorphisms (SNPs) array. After classical data cleaning, 261 individuals with 29849 markers (that is, SNPs) were kept.

We focus here on the tasseling time of maize, whose heritability is explained by many genes. We used two different implementations of Lasso for detecting the relevant markers: `glmnet` (Generalized Linear Models regularized by Lasso and elastic-NET, Friedman et al., 2010) and our own implementation, publicly available through the R package `quadrupen`<sup>3</sup>.

The two implementations were run using their default parameters, with the same penalty strength  $\lambda$ , selected by leave-one-out cross-validation with `glmnet`. The latter selected 169 markers among the 29849 SNPs, whereas `quadrupen` was more stringent, selecting only a subset of 156 markers. This notable difference is unexpected considering that the two implementations attempt to solve the very same convex optimization problem.

---

<sup>3</sup>The `quadrupen` package is available on the CRAN (Comprehensive R Archive Network <https://cran.r-project.org/web/packages/quadrupen/>)

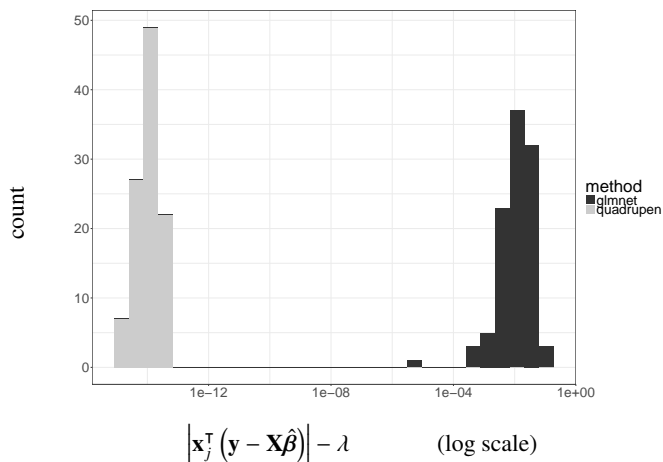


Figure 5: Histogram of the derivatives w.r.t. the non-zero coefficients of the parameter vectors returned by `glmnet` and `quadrupen`

In the following, we show how the speed and precision of `glmnet` are affected by the threshold controlling the stopping condition. Regarding precision, a first hint is provided in Figure 5, which displays the absolute value of the derivatives of the objective function with respect to the non-zero coefficients of the parameter vectors returned by `glmnet` and `quadrupen`, respectively. The departure from zero for `glmnet` illustrates its relative imprecision, which is responsible for the difference in the set of selected markers.

## 5.2. Synthetic data

We compare the performance of the proposed quadratic solver with representatives of the most successful competing algorithms. First, we use our own implementations of all competitors, so as to provide comparisons without implementation biases (language, library, etc.). We use R with most of the matrix calculus done in C++ using the `RcppArmadillo` package (Eddelbuettel and François, 2011; Sanderson, 2010) that relies on BLAS/LAPACK libraries for linear algebra operations. Second, we compare our code to the leading standalone packages that are available today, so as to provide comparisons avoiding a possible competence bias.

We use simulated data to obtain representative average results. Their generation covers the typical attributes of the real data encountered in post genomic and signal processing. In these domains, the main optimization difficulties result from ill-conditioning, which is either due to the high correlation between predictors, or to underdetermination when the number of variables exceeds the sample size (also known as the high-dimensional or the “large  $p$  small  $n$ ” setup). For the optimization algorithms based on active set strategies, bad conditioning is somehow alleviated when the objective function has a regular behavior when restricted to the subspace containing the solution. All other things being equal, this local conditioning is thus governed by the sparsity of the unknown true parameter (which affects the sparsity of the solution), which also heavily impacts the running times of most optimization algorithms available today.

### 5.2.1. Data Generation

The above-mentioned characteristics are explored without difficulty in the framework of linear regression. We generate samples of size  $n$  from the model

$$\mathbf{y} = \mathbf{X}\boldsymbol{\beta}^* + \boldsymbol{\varepsilon}, \quad \boldsymbol{\varepsilon} \sim \mathcal{N}(\mathbf{0}, \sigma^2 \mathbf{I}),$$

with  $\sigma$  chosen so as to reach a rather strong coefficient of determination ( $R^2 \approx 0.8$ ). The design matrix  $\mathbf{X}$  is drawn from a multivariate normal distribution in  $\mathbb{R}^p$ , and the conditioning of  $\mathbf{X}^T \mathbf{X}$  is ruled by the correlation between variables. We use the same correlation coefficient  $\rho$  for all pairs of variables. The sparsity of the true regression coefficients is controlled by a parameter  $s$ , with

$$\boldsymbol{\beta}^* = (\underbrace{2, \dots, 2}_{s/2}, \underbrace{-2, \dots, -2}_{s/2}, \underbrace{0, \dots, 0}_{p-s}).$$

Finally, the ratio  $p/n$  quantifies the well/ill-posedness of the problem.

### 5.2.2. Comparing Optimization Strategies

We compare here the performance of three state-of-the-art optimization strategies implemented in our own computational framework: accelerated proximal method (see, e.g., Beck and Teboulle, 2009), coordinate descent (popularized by Friedman et al., 2007), and our algorithm, that will respectively be named hereafter `proximal`, `coordinate` and `quadratic`. Our implementations estimate the solution to the elastic net problem

$$J_{\lambda_1, \lambda_2}^{\text{enet}}(\boldsymbol{\beta}) = \frac{1}{2} \|\mathbf{X}\boldsymbol{\beta} - \mathbf{y}\|_2^2 + \lambda_1 \|\boldsymbol{\beta}\|_1 + \frac{\lambda_2}{2} \|\boldsymbol{\beta}\|_2^2, \quad (7)$$

which is strictly convex when  $\lambda_2 > 0$  and thus admits a unique solution even if  $n < p$ .

The three implementations are embedded in the same active set routine, which approximately solves the optimization problem with respect to a limited number of variables as in Algorithm 1. They only differ regarding the inner optimization problem with respect to the current active variables, which is performed by an accelerated proximal gradient method for `proximal`, by coordinate descent for `coordinate`, and by the resolution of the worst-case quadratic problem for `quadratic`. We followed the practical recommendations of Bach et al. (2012) for accelerating the proximal and coordinate descent implementations, and we used the same halting condition for the three implementations, based on the approximate satisfaction of the first-order optimality conditions:

$$\max_{j \in \{1 \dots p\}} \left| \mathbf{x}_j^T (\mathbf{y} - \mathbf{X}\hat{\boldsymbol{\beta}}) + \lambda_2 \hat{\beta}_j \right| < \lambda_1 + \tau, \quad (8)$$

where the threshold  $\tau$  was fixed to  $\tau = 10^{-2}$  in our simulations.<sup>4</sup> Finally, the active set algorithm is itself wrapped in a warm-start routine, where the approximate solution to  $J_{\lambda_1, \lambda_2}^{\text{enet}}$  is used as the starting point for the resolution of  $J_{\lambda'_1, \lambda_2}^{\text{enet}}$  for  $\lambda'_1 < \lambda_1$ .

Our benchmark considers small-scale problems, with size  $p = 100$ , and the nine situations stemming from the choice of three following parameters:

- low, medium and high correlation between predictors ( $\rho \in \{0.1, 0.4, 0.8\}$ ),

<sup>4</sup>The rather loose threshold is favorable to `coordinate` and `proximal`, which reach the threshold, while `quadratic` ends up with a much smaller value, due to the exact resolution, up to machine precision, of the inner quadratic problem.

- low, medium and high-dimensional setting ( $p/n \in \{2, 1, 0.5\}$ ),
- low, medium and high levels of sparsity ( $s/p \in \{0.6, 0.3, 0.1\}$ ).

Each solver computes the elastic net for the tuning parameters  $\lambda_1$  and  $\lambda_2$  on a 2D-grid of  $50 \times 50$  values, and their running times have been averaged over 100 runs.

All results are qualitatively similar regarding the dimension and sparsity settings. Figure 6 displays the high-dimensional case ( $p = 2n$ ) with a medium level of sparsity ( $s = 30$ ) for the three levels of correlation. Each map represents the log-ratio between the timing of either `coordinate` or `proximal` versus `quadratic`, according to  $(\lambda_1, \lambda_2)$  for a given correlation level. Dark regions with a value of 1 indicate identical running times while lighter regions with a value of 10 indicate that `quadratic` is 10 times faster. Figure 6 illustrates that `quadratic` outperforms both `coordinate` and `proximal`, by running much faster in most cases, even reaching 300-fold speed increases. The largest gains are observed for small  $(\lambda_1, \lambda_2)$  penalty parameters for which the problem is ill-conditioned, including many active variables, resulting in a huge slowdown of the first-order methods `coordinate` and `proximal`. As the penalty parameters increase, smaller gains are observed, especially when  $\lambda_2$ , attached to the quadratic penalty, reaches high values for which all problems are well-conditioned, and where the elastic net is leaning towards univariate soft thresholding, in which case all algorithms behave similarly.

### 5.2.3. Comparing Stand-Alone Implementations

We now proceed to the evaluation of our code with three other stand-alone programs publicly available as R packages. We chose three leading state-of-the-art packages, namely `glmnet` (Generalized Linear Models regularized by Lasso and elastic-NET, Friedman et al., 2010), `lars` (Least Angle Regression, lasso and forward Stagewise, Efron et al., 2004) and `SPAMS` (SPARse Modeling Software, Bach et al., 2012), with two options `SPAMS-FISTA`, which implements an accelerated proximal method, and `SPAMS-LARS` which is a `lars` substitute. Note that `glmnet` does most of its internal computations in Fortran, `lars` in R, and `SPAMS` in C++.

We benchmark these packages by computing regularization paths for the Lasso<sup>5</sup>, that is, the elastic net Problem (7) with  $\lambda_2 = 0$ . The inaccuracy of the solutions produced is measured by the gap in the objective function compared to a reference solution, considered as being the true optimum. We use the `lars` solution as a reference, since it solves the Lasso problem up to the machine precision, relying on the LAPACK/BLAS routines. Furthermore, `lars` provides the solution path for the Lasso, that is, the set of solutions computed for each penalty parameter value for which variable activation or deletion occurs, from the empty model to the least-mean squares model. This set of reference penalty parameters is used here to define a sensible reproducible choice.

In high dimensional setups, the computational cost of returning the solutions for the largest models may be overwhelming compared to the one necessary for exploring the interesting part of the regularization path (Simon et al., 2011; Friedman et al., 2010). This is mostly due to numerical instability problems that may be encountered in these extreme settings, where the Lasso solution is overfitting as it approaches the set of solutions to the underdetermined least squares problem. We avoid a comparison mostly relying on these spurious cases by restricting the set of reference penalty parameters to the first  $\min(n, p)$  steps of `lars` (similar settings are used by Friedman et al., 2010).

---

<sup>5</sup>We benchmark the packages on a Lasso problem since the parametrization of the elastic net problem differs among packages, hindering fair comparisons.

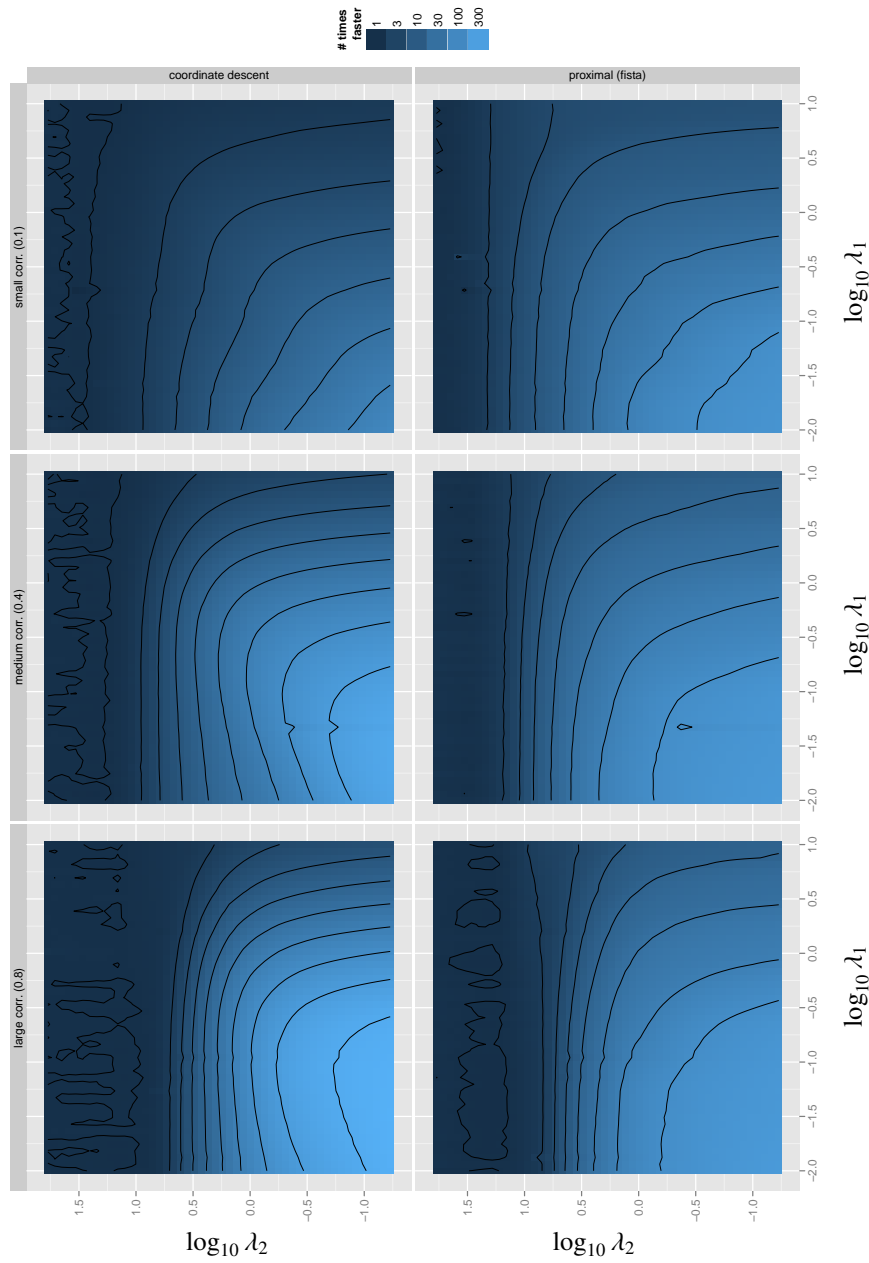


Figure 6: Log-ratio of computation times for coordinate (left), and proximal (right), versus quadratic, for  $(p, n) = (100, 50)$ ,  $s = 30$  and correlation  $\rho \in \{0.1, 0.4, 0.8\}$  (top, middle and bottom respectively).

Henceforth, the distance  $D$  of a given method to the optimum is evaluated on the whole set of penalties  $\Lambda$  used along the path, by

$$D(\text{method}) = \left( \frac{1}{|\Lambda|} \sum_{\lambda \in \Lambda} \left( J_{\lambda}^{\text{lasso}}(\hat{\beta}_{\lambda}^{\text{lars}}) - J_{\lambda}^{\text{lasso}}(\hat{\beta}_{\lambda}^{\text{method}}) \right)^2 \right)^{1/2},$$

where  $J_{\lambda}^{\text{lasso}}(\beta) = J_{\lambda,0}^{\text{enet}}(\beta)$  is the objective function of the Lasso evaluated at  $\beta$ , and  $\hat{\beta}_{\lambda}^{\text{method}}$  is the estimated optimal solution provided by the `method` package currently tested.

The data sets are generated according to the linear model described above, in three different high-dimensional settings and small to medium number of variables:  $(p, n) = (100, 40)$ ,  $(p, n) = (1000, 200)$  and  $(p, n) = (10000, 400)$ . The sparsity of the true underlying  $\beta^*$  is governed by  $s = 0.25 \min(n, p)$ , and the correlation between predictors is set by  $\rho \in \{0.1, 0.4, 0.8\}$ . For each value of  $\rho$ , we averaged the timings over 50 simulations, ensuring that each package computes the solutions at identical  $\lambda$  values, as defined above.

We pool together the runtimes obtained for the three levels of correlation for `quadrupen`, `SPAMS-LARS` and `lars`, which are not sensible to the correlation between features. In each plot of Figure 7, each of these methods is thus represented by a single point marking the average precision and the average distance to the optimum over the 150 runs (50 runs for each  $\rho \in \{0.1, 0.4, 0.8\}$ ). Note that for `lars` only the abscissa is meaningful since  $D(\text{lars})$  is zero by definition. Besides, `quadrupen`, which solves each quadratic problem up to the machine precision, tends to be within this precision of the `lars` solution. The `SPAMS-LARS` is also very precise, up to  $10^{-6}$ , which is the typical precision of the approximate resolution of linear systems. It is the fastest alternative for solving the Lasso when the problem is high-dimensional with a large number of variables (Figure 7, bottom-left).

In contrast, the (precision,timing)-values of `glmnet` and `SPAMS-FISTA` are highly affected by the threshold parameters<sup>6</sup> that control their stopping conditions. The computational burden to reach a given precision is also affected by the level of correlation, as illustrated in Figure 7. Obviously, a precise solution is difficult to reach with first-order descent algorithms in a high correlation setup, which corresponds to an ill-conditioned linear system. It may be surprising to observe that `SPAMS-FISTA` is about ten time slower than `glmnet`, as proximal and coordinate descent methods were experimentally shown to be roughly equivalent in our preceding analysis and by Bach et al. (2012). However, these two comparisons were carried out with the same active set strategy (that is, *with* active set for ours and *without* active set for Bach et al., 2012). We believe that this difference in the handling of active variables explains the relative bad performance of `SPAMS-FISTA`, which optimizes all variables along the regularization path, while `glmnet` uses a greedy active set strategy.

Overall, our implementation is highly competitive, that is, very accurate, at the `lars` level, and much faster. The speed improvements of `glmnet` are only observed for very rough approximate solutions and `SPAMS-FISTA` is dominated by `glmnet`. Our experiments, in the framework of active set methods, agree with the results of Bach et al. (2012): indeed, they observed that first-order methods are competitive with second-order ones only for low correlation levels and small

---

<sup>6</sup>In `glmnet`, convergence is monitored by the stability of the objective function, measured between two optimization steps, and optimization is halted when changes fall below the specified threshold (scaled by the null deviance). In `SPAMS-FISTA`, the stopping condition of the algorithm is based on the relative change of parameters between two iterations.

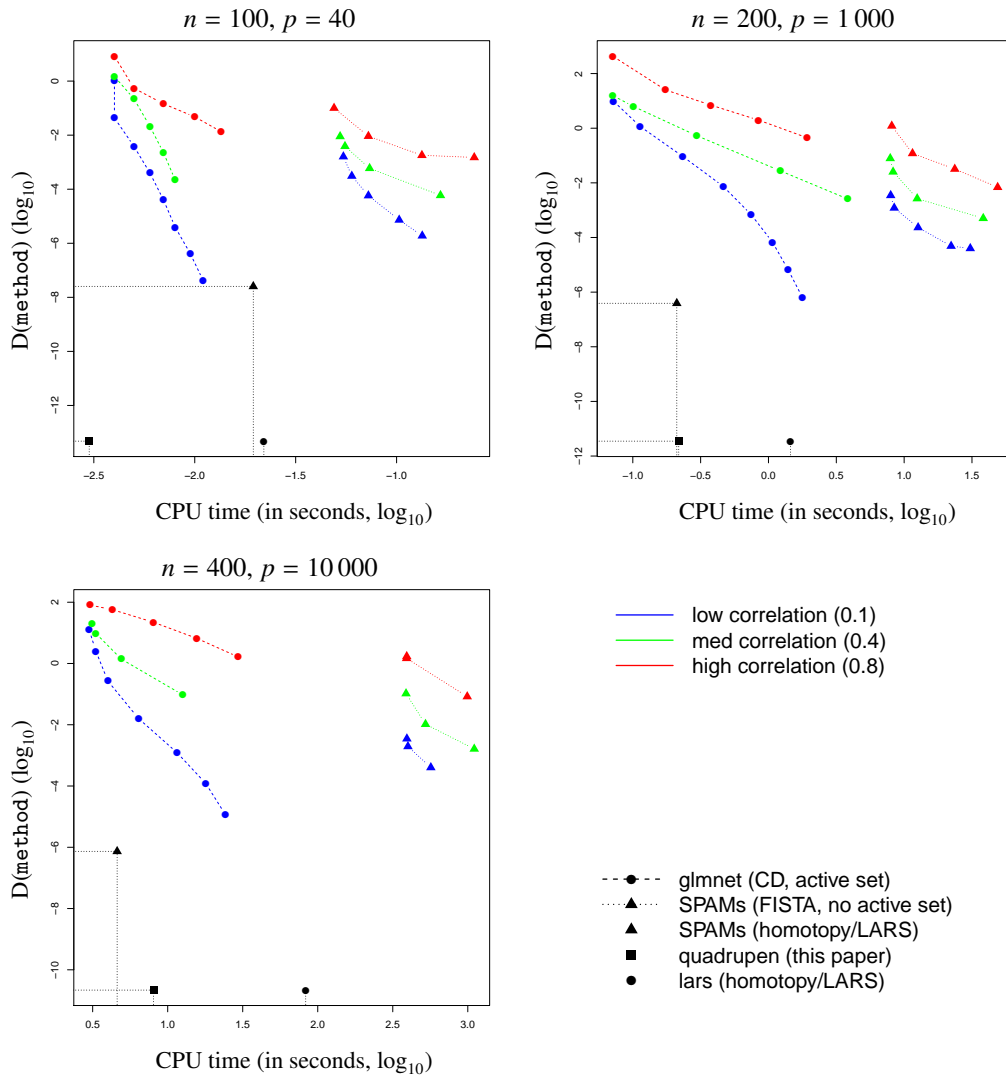


Figure 7: Distance to optimum versus CPU time for three different high-dimensional settings:  $(p, n) = (100, 40)$  (top left),  $(p, n) = (1000, 200)$  (top right) and  $p = (10000, 400)$  (bottom left).

penalties (which entails a large number of active variables). Conversely, our results may appear to contradict some of the experimental findings of Friedman et al. (2010): first, we observe that `glmnet` is quite sensitive to correlations, and second, the optimized second-order methods are competitive with `glmnet`. These differences in conclusions arise from the differences in experimental protocols: while we compare running times at a given accuracy, they are compared at a given threshold on the stopping criterion by Friedman et al. (2010). Regarding the influence of correlations, the stability-based criterion can be fooled due to the tiny step size that typically occurs for ill-conditioned problems, leading to a sizable early stopping. Regarding the second point, even though the R implementation of `lars` may indeed be slow compared to `glmnet`, considerable improvements can be obtained using optimized second-order methods such as `quadrupen` as soon as a sensible accuracy is required, especially when correlation increases.

Finally, among the accurate solvers, `SPAMS-LARS` is insignificantly less accurate than `quadrupen` or `lars` in a statistical context. It is always faster than `lars` and slightly faster than `quadrupen` for the largest problem sizes (Figure 7, bottom-left) and much slower for the smallest problem (Figure 7, top-left).

#### 5.2.4. Link between accuracy of solutions and prediction performances

When the “irrepresentable condition” (Zhao and Yu, 2006) holds, the Lasso should select the true model consistently. However, even when this rather restrictive condition is fulfilled, perfect support recovery obviously requires numerical accuracy: rough estimates may speed up the procedure, but whatever optimization strategy is used, stopping an algorithm is likely to prevent either the removal of all irrelevant coefficients or the insertion of all relevant ones. The support of the solution may then be far from the optimal one.

We advocate here that our quadratic solver is very competitive in computation time when support recovery matters, that is, when high level of accuracy is needed, in small (few hundreds of variables) and medium sized problems (few thousands). As an illustration, we generate 100 data sets under the linear model described above, with a rather strong coefficient of determination ( $R^2 \approx 0.8$  on average), a rather high level of correlation between predictors ( $\rho = 0.8$ ) and a medium level of sparsity ( $s/p = 30\%$ ). The number of variable is kept low ( $p = 100$ ) and the difficulty of the estimation problem is tuned by the  $n/p$  ratio. For each data set, we also generate a test set sufficiently large (say,  $10n$ ) to evaluate the quality of the prediction without depending on any sampling fluctuation. We compare the Lasso solutions computed by `quadrupen` to the ones returned by `glmnet` with various level of accuracy<sup>7</sup>. Figure 8 reports performances, as measured by the mean squared test error and the support error rate.

As expected, the curves show that selecting variables and searching for the best prediction are two different problems. The selection problem (bottom of Figure 8) always requires a sparser model than the prediction problem. But despite this obvious difference, the more accurate the solution returned by the algorithm, the better the performances for any levels of penalty and for both performance measures.

Now focusing on `glmnet` performances, the better the accuracy, the smaller the MSE and the support error rate. But the better the accuracy, the slower the algorithm becomes. Using the default settings allows to have a result very close to our quadratic solver, and the performance differences become negligible between our approach and `glmnet` running with high precision.

---

<sup>7</sup>This is done via the `thresh` argument of the `glmnet` procedure, whose default value is  $1e-7$ . In our experiments, `low`, `med` and `high` level of accuracy for `glmnet` respectively correspond to `thresh` set to  $1e-1$ ,  $1e-4$ , and  $1e-9$ .

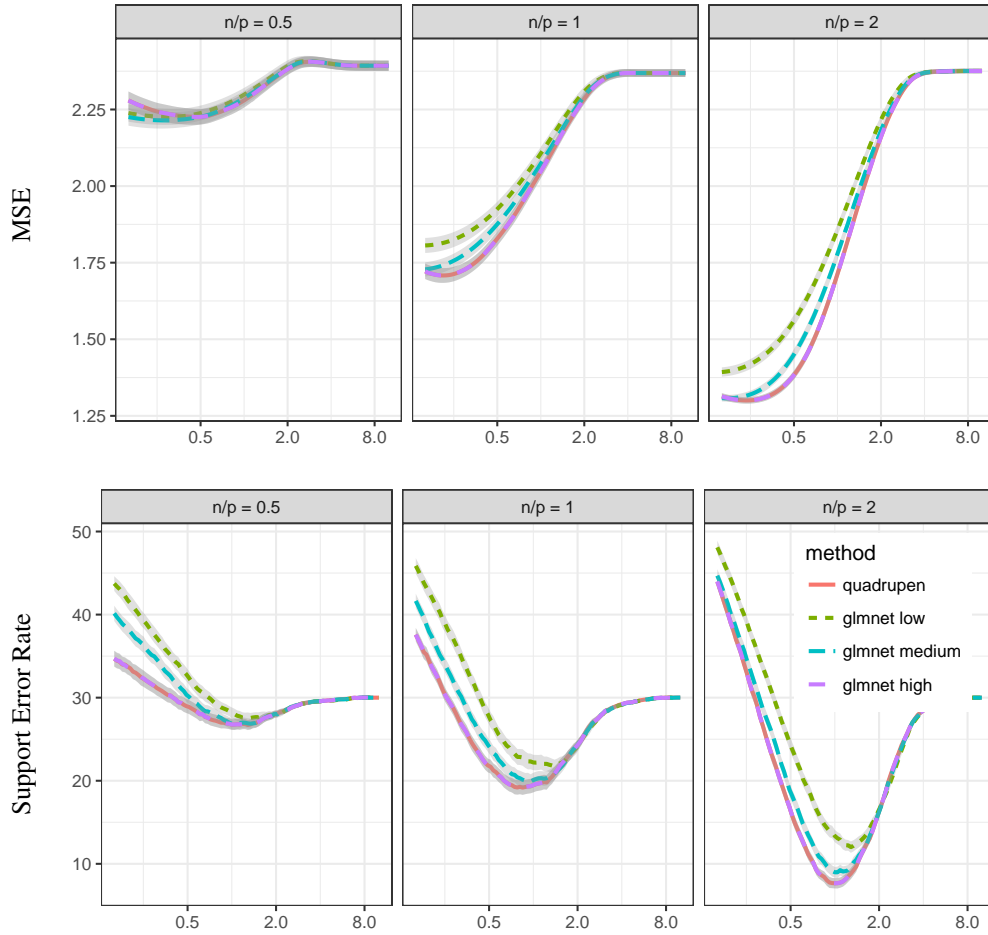


Figure 8: Test performances according to the penalty parameter for the Lasso estimates returned by `quadrupen` and `glmnet` at various level of accuracy. Three high-dimensional setups are illustrated: from left to right  $n/p = 1/2$ ,  $n/p = 1$  and  $n/p = 2$ ; top: mean squared test error; bottom: support error rate.

methods	quadrupen	glmnet low	glmnet med	glmnet high
timing (ms)	8	7	8	64
accuracy (dist. to opt.)	$5.9 \times 10^{-14}$	$7.2 \times 10^0$	$6.04 \times 10^0$	$1.47 \times 10^{-2}$

Table 1: Median timings and solution accuracies

However, Table 1 illustrates that high accuracy is achieved at a high computational cost: to be at par with quadrupen with regards to test performances, `glmnet` is about ten times slower than our solver.

## 6. Discussion

This paper presents a new viewpoint on sparsity-inducing penalties where the dual norms associated with these penalties play a central role. Technically, our formulation is a simple dual form of the original problem. However, we do not follow a very general principle such as Fenchel duality: we specifically tailor our formulation to optimization problems involving a sparsity-inducing norm. The dual variables define a series of linear or quadratic penalties whose sublevel sets define the feasible set of the original problem through intersection.

This viewpoint enables to encompass in the same framework several well-known penalties. In particular, we detailed how the solutions to the Lasso and the group-Lasso (with the  $\ell_{\infty,1}$  mixed norm), possibly applied together with an  $\ell_2$  ridge penalty (leading to what is known as the elastic net for the Lasso) can be derived.

We derived a general-purpose algorithm that computes the solution to the penalized regression problem, and proposed a new lower bound on the minimum of the objective function to assess convergence. The proposed algorithm solves a series of quadratic problems on a working set defined by the dual variables. It has been thoroughly tested and compared with state-of-the-art implementations for the elastic net and the Lasso, and prevails over its competitors for the problems tested, involving up to a few thousands of variables.

From a practical viewpoint, an important feature of our approach is that it solves the original problem up to machine precision: we shown that when variable selection is involved, optimization with a high level of precision is mandatory to recover the true model.

Regarding future development, the algorithm can be adapted to non-quadratic loss functions for addressing other learning problems such as classification, but this generalization, which requires solving non-quadratic problems, may not be as efficient compared to the existing alternatives. We are now examining how to address a wider range of penalties by extending the framework in two directions: first, to accommodate additional general  $\ell_2$  penalties in the form of arbitrary symmetric positive semidefinite matrix instead of the simple ridge, in particular to provide an efficient implementation of the structured elastic net (Slawski et al., 2010) ; second, we plan to derive similar views on a wider range of sparsity-inducing penalties, such as the fused-Lasso or the OSCAR (Bondell and Reich, 2008).

## References

- Ambroise, C., McLachlan, G. J., 2002. Selection bias in gene extraction on the basis of microarray gene-expression data. *Proceedings of the National Academy of Sciences* 99 (10), 6562–6566.
- Bach, F., Jenatton, R., Mairal, J., Obozinski, G., 2012. Optimization with sparsity-inducing penalties. *Foundations and Trends in Machine Learning* 4 (1), 1–106.
- Beck, A., Teboulle, M., 2009. Fast iterative shrinkage-thresholding algorithm for linear inverse problems. *SIAM Journal on Imaging Sciences* 2, 183–202.
- Bondell, H. D., Reich, B. J., 2008. Simultaneous regression shrinkage, variable selection, and supervised clustering of predictors with oscar. *Biometrics* 64 (1), 115–123.
- Bonnans, J. F., Gilbert, J. C., Lemaréchal, C., Sagastizábal, C., 2006. *Numerical Optimization: Theoretical and Practical Aspects*, 2nd Edition. Springer.

- Bottou, L., Bousquet, O., 2008. The tradeoffs of large scale learning. In: Platt, J. C., Koller, D., Singer, Y., Roweis, S. (Eds.), *Advances in Neural Information Processing Systems*, 20 (NIPS 2008). pp. 161–168.
- Boyd, S., Parikh, N., Chu, E., Peleato, B., Eckstein, J., 2011. Distributed optimization and statistical learning via the alternating direction method of multipliers. *Foundations and Trends in Machine Learning* 3 (1), 1–122.
- Boyd, S., Vandenberghe, L., 2004. *Convex optimization*. Cambridge university press.
- Eddelbuettel, D., François, R., 4 2011. Rcpp: Seamless R and C++ integration. *Journal of Statistical Software* 40 (8), 1–18.  
URL <http://www.jstatsoft.org/v40/i08>
- Efron, B., Hastie, T., Johnstone, I., Tibshirani, R., 2004. Least angle regression. *The Annals of Statistics* 32 (2), 407–499, with discussion, and a rejoinder by the authors.
- Freedman, D. A., 1983. A note on screening regression equations. *The American Statistician* 37 (2), 152–155.
- Friedman, J., Hastie, T., Höfling, H., Tibshirani, R., 2007. Pathwise coordinate optimization. *The Annals of Applied Statistics* 1 (2), 302–332.
- Friedman, J. H., Hastie, T., Tibshirani, R., 2 2010. Regularization paths for generalized linear models via coordinate descent. *Journal of Statistical Software* 33 (1), 1–22.  
URL <http://www.jstatsoft.org/v33/i01>
- Gilbert, J. C., 2016. *Fragments d’optimisation différentiable – théorie et algorithmes*.  
URL <http://www-rocq.inria.fr/~gilbert/ensta/optim.html>
- Grandvalet, Y., Canu, S., 1999. Outcomes of the equivalence of adaptive ridge with least absolute shrinkage. In: *Advances in Neural Information Processing Systems* 11 (NIPS 1998). pp. 445–451.
- Lacoste-Julien, S., Jaggi, M., Schmidt, M., Pletscher, P., 2012. Block-coordinate Frank-Wolfe optimization for structural svms. arXiv preprint arXiv:1207.4747.
- Mairal, J., 2010. *Sparse coding for machine learning, image processing and computer vision*. Ph.D. thesis, École Normale Supérieure de Cachan.
- Moulines, E., Bach, F. R., 2011. Non-asymptotic analysis of stochastic approximation algorithms for machine learning. In: *Advances in Neural Information Processing Systems*. pp. 451–459.
- Osborne, M. R., Presnell, B., Turlach, B. A., 2000. On the LASSO and its dual. *Journal of Computational and Graphical Statistics* 9 (2), 319–337.
- Rincent, R., Moreau, L., Monod, H., Kuhn, E., Melchinger, A., Malvar, R., Moreno-Gonzalez, J., Nicolas, S., Madur, D., Combes, V., Dumas, A., Altmann, T., Brunel, D., Ouzunova, M., Flament, P., Dubreuil, P., Charcosset, A., Mary-Huard, T., 2014. Recovering power in association mapping panels with variable levels of linkage disequilibrium. *Genetics* 197 (1), 375–387.
- Sanderson, C., 2010. *Armadillo: An open source C++ linear algebra library for fast prototyping and computationally intensive experiments*. Tech. rep., NICTA.  
URL <http://http://arma.sourceforge.net/>
- Simon, N., Friedman, J. H., Hastie, T., Tibshirani, R., 3 2011. Regularization paths for cox’s proportional hazards model via coordinate descent. *Journal of Statistical Software* 39 (5), 1–13.  
URL <http://www.jstatsoft.org/v39/i05>
- Slawski, M., zu Castell, W., Tutz, G., 2010. Feature selection guided by structural information. *The Annals of Applied Statistics* 4 (2), 1056–1080.
- Turlach, B. A., Venables, W. N., Wright, S. J., 2005. Simultaneous variable selection. *Technometrics* 47 (3), 349–363.
- Zhao, P., Yu, B., 2006. On model selection consistency of lasso. *Journal of Machine Learning Research* 7, 2541–2567.
- Zou, H., Hastie, T., 2005. Regularization and variable selection via the elastic net. *Journal of the Royal Statistical Society: Series B (Statistical Methodology)* 67 (2), 301–320.

## Appendix A. Proof of Proposition 1

We detail here a proof yielding a slightly tighter bound. Proposition 1 is simply a corollary of Proposition 2 stated and proved below.

The following Lemma relates the penalty associated with a infeasible  $\gamma$ -value ( $\|\gamma\|_* > \eta$ ) to the one obtained by shrinking this  $\gamma$ -value to reach the boundary of  $\mathcal{B}_*^!$ .

**Lemma 1.** *Let  $\mathcal{S} \subseteq \{1, \dots, p\}$ ,  $\alpha \in (0, 1)$ ,  $\|\cdot\|_*$  be a vectorial norm and  $\varphi^*(\cdot, \mathcal{S}, \alpha) : \mathbb{R}^p \rightarrow \mathbb{R}^p$  be defined as follows:*

$$\begin{cases} \varphi_{\mathcal{S}}^*(\gamma, \mathcal{S}, \alpha) = \gamma_{\mathcal{S}} \\ \varphi_{\mathcal{S}^c}^*(\gamma, \mathcal{S}, \alpha) = \alpha \gamma_{\mathcal{S}^c} \end{cases} .$$

Then,

$$\|\boldsymbol{\beta} - \varphi^*(\boldsymbol{\gamma}, \mathcal{S}, \alpha)\|_2^2 \geq \alpha \|\boldsymbol{\beta} - \boldsymbol{\gamma}\|_2^2 - \alpha(1 - \alpha) \|\boldsymbol{\gamma}_{\mathcal{S}^c}\|_2^2 . \quad (\text{A.1})$$

*Proof.*

$$\begin{aligned} \|\boldsymbol{\beta} - \varphi^*(\boldsymbol{\gamma}, \mathcal{S}, \alpha)\|_2^2 &= \|\boldsymbol{\beta}_{\mathcal{S}} - \boldsymbol{\gamma}_{\mathcal{S}}\|_2^2 + \alpha \|\boldsymbol{\beta}_{\mathcal{S}^c} - \boldsymbol{\gamma}_{\mathcal{S}^c}\|_2^2 + (1 - \alpha) \|\boldsymbol{\beta}_{\mathcal{S}^c}\|_2^2 - \alpha(1 - \alpha) \|\boldsymbol{\gamma}_{\mathcal{S}^c}\|_2^2 \\ &\geq \|\boldsymbol{\beta}_{\mathcal{S}} - \boldsymbol{\gamma}_{\mathcal{S}}\|_2^2 + \alpha \|\boldsymbol{\beta}_{\mathcal{S}^c} - \boldsymbol{\gamma}_{\mathcal{S}^c}\|_2^2 - \alpha(1 - \alpha) \|\boldsymbol{\gamma}_{\mathcal{S}^c}\|_2^2 \\ &\geq \alpha \|\boldsymbol{\beta} - \boldsymbol{\gamma}\|_2^2 - \alpha(1 - \alpha) \|\boldsymbol{\gamma}_{\mathcal{S}^c}\|_2^2 . \end{aligned}$$

□

**Proposition 2.** For any vectorial norm  $\|\cdot\|_*$ ,  $\forall \boldsymbol{\gamma} \in \mathbb{R}^p : \|\boldsymbol{\gamma}\|_* \geq \eta$ , and  $\forall (\mathcal{S}, \alpha) \in 2^{\{1, \dots, p\}} \times (0, 1)$  such that  $\|(\boldsymbol{\gamma}_{\mathcal{S}}, \alpha \boldsymbol{\gamma}_{\mathcal{S}^c})\|_* \leq \eta$ , we have:

$$\min_{\boldsymbol{\beta} \in \mathbb{R}^p} \max_{\boldsymbol{\gamma}' \in \mathcal{B}_*^{\eta}} J_{\lambda}(\boldsymbol{\beta}, \boldsymbol{\gamma}') \geq \alpha J_{\lambda}(\boldsymbol{\beta}^*(\boldsymbol{\gamma}), \boldsymbol{\gamma}) - \lambda \alpha(1 - \alpha) \|\boldsymbol{\gamma}_{\mathcal{S}^c}\|_2^2 ,$$

where

$$J_{\lambda}(\boldsymbol{\beta}, \boldsymbol{\gamma}) = \|\mathbf{X}\boldsymbol{\beta} - \mathbf{y}\|_2^2 + \lambda \|\boldsymbol{\beta} - \boldsymbol{\gamma}\|_2^2 \quad \text{and} \quad \boldsymbol{\beta}^*(\boldsymbol{\gamma}) = \arg \min_{\boldsymbol{\beta} \in \mathbb{R}^p} J_{\lambda}(\boldsymbol{\beta}, \boldsymbol{\gamma}) .$$

*Proof.* For all  $\boldsymbol{\beta} \in \mathbb{R}^p$  and for any  $(\boldsymbol{\gamma}, \mathcal{S}, \alpha) \in \mathbb{R}^p \times 2^{\{1, \dots, p\}} \times (0, 1)$  such that  $\varphi^*(\boldsymbol{\gamma}, \mathcal{S}, \alpha) \in \mathcal{B}_*^{\eta}$ , with  $\varphi^*$  defined as in Lemma 1 we have

$$\max_{\boldsymbol{\gamma}' \in \mathcal{B}_*^{\eta}} J_{\lambda}(\boldsymbol{\beta}, \boldsymbol{\gamma}') \geq J_{\lambda}(\boldsymbol{\beta}, \varphi^*(\boldsymbol{\gamma}, \mathcal{S}, \alpha)) , \quad (\text{A.2})$$

since  $\varphi^*(\boldsymbol{\gamma}, \mathcal{S}, \alpha)$  belongs to  $\mathcal{B}_*^{\eta}$ . We now compute a lower bound of the right-hand-side for  $\boldsymbol{\gamma}$  such that  $\|\boldsymbol{\gamma}\|_* \geq \eta$ :

$$\begin{aligned} J_{\lambda}(\boldsymbol{\beta}, \varphi^*(\boldsymbol{\gamma}, \mathcal{S}, \alpha)) &= \alpha \left( \frac{1}{\alpha} \|\mathbf{X}\boldsymbol{\beta} - \mathbf{y}\|_2^2 + \frac{\lambda}{\alpha} \|\boldsymbol{\beta} - \varphi^*(\boldsymbol{\gamma}, \mathcal{S}, \alpha)\|_2^2 \right) \\ &\geq \alpha \left( \|\mathbf{X}\boldsymbol{\beta} - \mathbf{y}\|_2^2 + \frac{\lambda}{\alpha} \|\boldsymbol{\beta} - \varphi^*(\boldsymbol{\gamma}, \mathcal{S}, \alpha)\|_2^2 \right) \\ &\geq \alpha \left( \|\mathbf{X}\boldsymbol{\beta} - \mathbf{y}\|_2^2 + \lambda \|\boldsymbol{\beta} - \boldsymbol{\gamma}\|_2^2 \right) - \lambda \alpha(1 - \alpha) \|\boldsymbol{\gamma}_{\mathcal{S}^c}\|_2^2 , \end{aligned} \quad (\text{A.3})$$

where the last inequality stems from Lemma 1. This inequality holds for any given  $\boldsymbol{\beta}$ -value, in particular for  $\boldsymbol{\beta}^*(\varphi^*(\boldsymbol{\gamma}, \mathcal{S}, \alpha)) = \arg \min_{\boldsymbol{\beta} \in \mathbb{R}^p} J_{\lambda}(\boldsymbol{\beta}, \varphi^*(\boldsymbol{\gamma}, \mathcal{S}, \alpha))$ :

$$\begin{aligned} \min_{\boldsymbol{\beta} \in \mathbb{R}^p} J_{\lambda}(\boldsymbol{\beta}, \varphi^*(\boldsymbol{\gamma}, \mathcal{S}, \alpha)) &\geq \alpha J_{\lambda}(\boldsymbol{\beta}^*(\varphi^*(\boldsymbol{\gamma}, \mathcal{S}, \alpha))) - \lambda \alpha(1 - \alpha) \|\boldsymbol{\gamma}_{\mathcal{S}^c}\|_2^2 \\ &\geq \alpha J_{\lambda}(\boldsymbol{\beta}^*(\boldsymbol{\gamma}), \boldsymbol{\gamma}) - \lambda \alpha(1 - \alpha) \|\boldsymbol{\gamma}_{\mathcal{S}^c}\|_2^2 , \end{aligned} \quad (\text{A.4})$$

where the second inequality follows from the definition of  $\boldsymbol{\beta}^*(\boldsymbol{\gamma})$ . Inequality (A.4) can be restated as:

$$\min_{\boldsymbol{\beta} \in \mathbb{R}^p} J_{\lambda}(\boldsymbol{\beta}, \varphi^*(\boldsymbol{\gamma}, \mathcal{S}, \alpha)) \geq \alpha \min_{\boldsymbol{\beta} \in \mathbb{R}^p} J_{\lambda}(\boldsymbol{\beta}, \boldsymbol{\gamma}) - \lambda \alpha(1 - \alpha) \|\boldsymbol{\gamma}_{\mathcal{S}^c}\|_2^2 .$$

We finally remark that, since  $\varphi^*(\boldsymbol{\gamma}, \mathcal{S}, \alpha) \in \mathcal{B}_*^{\eta}$ , we trivially have:

$$\min_{\boldsymbol{\beta} \in \mathbb{R}^p} \max_{\boldsymbol{\gamma} \in \mathcal{B}_*^{\eta}} J_{\lambda}(\boldsymbol{\beta}, \boldsymbol{\gamma}) \geq \min_{\boldsymbol{\beta} \in \mathbb{R}^p} J_{\lambda}(\boldsymbol{\beta}, \varphi^*(\boldsymbol{\gamma}, \mathcal{S}, \alpha)) ,$$

which concludes the proof. □

Proposition 1 follows by choosing  $\alpha = \eta / \|\boldsymbol{\gamma}\|_*$ .